Hindawi Publishing Corporation
Journal of Nanomaterials
Volume 2013, Article ID 653892, 10 pages
http://dx.doi.org/10.1155/2013/653892

Research Article

Physicochemical Properties and *In Vitro* Cytotoxicity Studies of Chitosan as a Potential Carrier for Dicer-Substrate siRNA

Maria Abdul Ghafoor Raja,[1] Haliza Katas,[1] Zariyantey Abd Hamid,[2] and Nur Atiqah Razali[1]

[1] *Centre for Drug Delivery Research, Faculty of Pharmacy, Universiti Kebangsaan Malaysia, Jalan Raja Muda Abdul Aziz, 50300 Kuala Lumpur, Malaysia*
[2] *Program of Biomedical Science, School of Diagnostic and Applied Health Sciences, Faculty of Health Sciences, Universiti Kebangsaan Malaysia, Jalan Raja Muda Abdul Aziz, 50300 Kuala Lumpur, Malaysia*

Correspondence should be addressed to Haliza Katas; haliz12@hotmail.com

Received 17 May 2013; Revised 26 July 2013; Accepted 27 July 2013

Academic Editor: Hongchen Chen Gu

Recently, Dicer-substrate small interfering RNA (DsiRNA) has gained attention owing to its greater potency over small interfering RNA (siRNA). However, the use of DsiRNA is restricted by its rapid degradation *in vitro*. To address this issue, chitosan nanoparticulate deliver yplatform for the Dicer-substrate siRNA (DsiRNA) was developed and characterized. Nanoparticles were prepared by simple complexation and ionic gelation methods. The mean particle size of DsiRNA-adsorbed chitosan nanospheres (DsiRNA-CS NPs) prepared by the ionic gelation method ranged from 225 to 335 nm, while simple complexation yielded DsiRNA-chitosan complexes (DsiRNA-CS complexes) ranging from 270 to 730 nm. The zeta potential of both types of nanoparticles ranged from +40 to +65 mV. TEM and AFM micrographs revealed spherical and irregular morphology of DsiRNA-CS NPs and DsiRNA-CS complexes. ATR-FTIR spectroscopy confirmed the presence of DsiRNA in the CS NPs/complexes. Both types of nanoparticles exhibited sustained release and high binding and encapsulation (100%) efficiency of DsiRNA. DsiRNA-CS NPs/complexes showed low, concentration-dependent cytotoxicity *in vitro*. DsiRNA-CS NPs showed better stability than the complexes when stored at 4 and 25°C. Thus, it is anticipated that CS NPs are promising vectors for DsiRNA delivery due to their stability, safety, and cost-effectiveness.

1. Introduction

Successful gene delivery and expression remain a major difficulty that must be overcome before genetic therapies gain clinical acceptance. There are, however, barriers to effective delivery of these molecules, as most nucleic acids are quickly degraded and cleared by nucleases and macrophages. Therefore, a degree of protection is required for incorporation into their delivery system [1]. Currently, there is much emphasis on the further development of nucleic acid delivery systems.

Viral and nonviral vectors have been used as gene delivery carriers. Even though viral vectors have higher transfection efficiencies in most cells, safety concerns were raised in numerous clinical trials [2]. Nonviral vectors have garnered much consideration owing to their ease of synthesis and modification, low immunogenicity, and controllable size [3]. Positively charged cationic polymers can effectively bind to and protect nucleic acids such as DNA, oligonucleotides, and siRNAs. Nonviral delivery systems using cationic liposomes and polymers, such as polyethylenimine (PEI), poly(L-lysine) (PLL), and their respective derivatives, have been used to condense plasmid DNA (pDNA) or siRNA to form nanoparticles [4–6]. However, liposomal-based formulations normally leading to cell toxicity [7] are quickly cleared from the bloodstream [8]. Among all the recent materials used for polymeric nanoparticles synthesis, chitosan (CS), a natural plentiful biopolymer obtained by chitin deacetylation, has gained considerable interest [9]. CS is a linear polysaccharide composed of glucosamine and N-acetyl glucosamine residues and can be derived by partial deacetylation of chitin [10]. CS is known to be biocompatible, less toxic, nonimmunogenic, and degradable by enzymes [11–13]. CS has been used extensively in many drug delivery applications, especially in gene delivery systems, because of its positively charged amines that allow

electrostatic interactions with negatively charged nucleic acids to form stable complexes [14, 15]. CS has been studied for more than a decade as a gene vector for pDNA, oligonucleotides [16], and siRNA [17]. In recent years, low molecular weight (LMW) CS nanoparticles have shown great potential in the applications of drug delivery and nonviral vector for gene delivery. This is because, compared with high molecular weight (HMW) chitosan, LMW chitosan shows better solubility, biocompatibility, bioactivity, biodegradability, and even less toxicity [18]. To our knowledge, until now there have been no studies investigating the use of LMW CS to deliver the Dicer-substrate siRNA (DsiRNA) *in vitro* or *in vivo*.

In 2005, some groups used slightly longer synthetic RNAs that are substrates for Dicer and that are more potent than traditional 21-mer siRNAs [19, 20]. These longer RNAs are processed by Dicer into 21-mer siRNAs in a predictable manner, [21] and the augmented potency seen with this strategy is thought to arise from the participation of Dicer in RNA-induced silencing complex formation. Characteristically, these reagents are synthetic RNA duplexes that are 27 bases in length and are referred to as DsiRNAs.

In the current study, LMW CS was used, and two methods of DsiRNA association were studied: by simple complexation and adsorption of DsiRNA onto the surface of preformed CS nanospheres (CS NPs). To address the lack of information regarding the interactions between DsiRNA and CS, since DsiRNA's structure and size are relatively different from those of siRNA, these systems were characterized in terms of their physical (particle size and distribution, surface charge, and morphology) and biological features (cytotoxicity). The efficiency of DsiRNA encapsulation, binding, and storage stability was also studied.

2. Experimental

2.1. Materials. Low molecular weight CS of molecular weight (MW) 190 kDa with a 75–85% degree of deacetylation (DD) was obtained from Sigma-Aldrich (USA), and pentasodium tripolyphosphate (TPP) was obtained from Merck (Germany). DsiRNA targeting the VEGF gene [5′-rGrGrA rGrUrA rCrCrC rUrGrA rUrGrA rGrArU rCrGrA rGrUA C-3′ (sense strand) and 5′-rGrUrA rCrUrC rGrArU rCrUrC rArUrC rArGrG rGrUrA rCrUrC rCrCrA-3′ (antisense strand)] was purchased from Integrated DNA Technologies (IDT), USA. Chinese hamster lung fibroblast (V79) cell lines and human colorectal adenocarcinoma cells (DLD-1) were obtained from American Type Culture Collection (ATCC, Manassas, USA). Dulbecco's Modified Eagle's Medium (DMEM), fetal bovine serum (FBS), phosphate buffered saline (PBS), and penicillin-streptomycin (pen-strep) were purchased from Gibco (USA). The alamarBlue reagent was purchased from Invitrogen (USA). Acetic acid and other chemicals used were of analytical grade.

2.2. Preparation of DsiRNA-CS Nanoparticles

2.2.1. Simple Complexation. Four different concentrations of CS solution (0.1%, 0.2%, 0.3%, and 0.4% w/v) were prepared by diluting chitosan stock solution with deionized water containing 2% v/v glacial acetic acid. CS-DsiRNA complexes were prepared by adding CS solution dropwise to an equal volume of DsiRNA solution (15 μg/mL in deionized water) (Figure 1(a)). The mixture was quickly mixed by inverting the reaction tube up and down for a few seconds and incubating for 30 min at room temperature before further analysis.

2.2.2. Ionic Gelation. CS NPs were prepared *via* the ionic gelation method established by Calvo et al. [22] with some modifications. CS solutions (0.1%, 0.2%, 0.3%, and 0.4% w/v) were prepared by dissolving CS in 2% v/v glacial acetic acid. TPP solution (1 mg/mL) was prepared by dissolving in deionized water. NPs were formed by adding 1.2 mL of TPP aqueous solution dropwise into 3 mL CS solution (0.4%, 0.3%, 0.2%, and 0.1% w/v) with constant magnetic stirring (MS MP8 Wise Stir Wertheim, Germany) at 700 revolutions per minute (rpm) for 30 min at room temperature and incubated at room temperature for 30 min before further analysis. NPs were collected by centrifugation (Optima L-100 XP Ultracentrifuge, Beckman-Coulter, California, USA) at a speed of 35,000 rpm at 10°C for 30 min. The supernatants were discarded, and the NPs were resuspended in filtered (Millex GP filter unit, Millipore, 0.25 μm) deionized water. Then, DsiRNA was adsorbed onto the surface of CS NPs by adding 500 μL of DsiRNA solution (15 μg/mL) dropwise into 500 μL of CS NP suspension and quickly mixed by inverting the reaction tube up and down for a few seconds (Figure 1(b)). Finally, the particles were incubated for 2 h at room temperature before further analysis.

2.2.3. ATR-FTIR Spectroscopic Analysis. The ATR-FTIR spectra of naked DsiRNA, CS, TPP, DsiRNA-CS NPs/complexes, and blank CS NPs were recorded against the background by using a universal ATR sampling assembly (Spectrum 100; PerkinElmer, Waltham, MA, USA). For each sample, 16 scans were obtained at a resolution of 4 cm^{-1} in the range of 4000 to 600 cm^{-1}.

2.2.4. Determination of Particle Size and Zeta Potential. Mean particle size, polydispersity index (PDI), and zeta potential of CS NPs were measured on a ZS-90 Zetasizer (Malvern Instruments, Worcestershire, UK) that was based on photon correlation spectroscopy (PCS).

2.2.5. Morphological Analysis. Morphological characterization of DsiRNA-CS NPs, complexes was carried out by using transmission electron microscopy (TEM), Tecnai Spirit, FEI, Eindhoven (The Netherlands), and atomic force microscopy (AFM) NTEGRA Prima device (NT-MDT, Russia).

2.2.6. Determination of DsiRNA Encapsulation Efficiency. The encapsulation efficiency (%) of DsiRNA complexed with CS or adsorbed onto CS NPs was measured by using UV-Vis spectrophotometer (Shimadzu 1800) at 260 nm from the following formula:

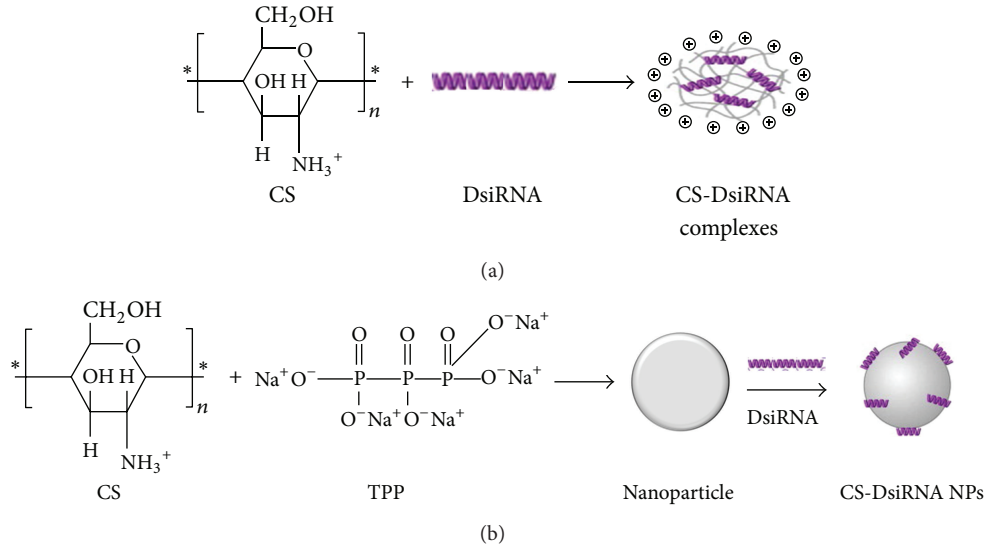

Figure 1: Representation of CS nanoparticles prepared by simple complexation (a) and ionic gelation methods (b).

$$\frac{(\text{Concentration of DsiRNA added} - \text{Concentration of DsiRNA in supernatant})}{(\text{Concentration of DsiRNA added})} \times 100. \quad (1)$$

2.2.7. Gel Retardation Assay. The binding of DsiRNA to CS was determined on a 4% w/v agarose gel with SYBR Green (Invitrogen). A series of different CS to DsiRNA weight ratios (20 μL of sample containing 0.15 μg of DsiRNA), prepared by both methods, were loaded into the wells. The DsiRNA bands were then visualized by using a real-time UV transilluminator (Invitrogen, USA).

2.2.8. Determination of Storage Stability. In order to investigate the storage stability of DsiRNA-CS NPs/complexes (prepared from 0.3% w/v of CS), the mean diameter of DsiRNA loaded CS NPs/complexes in deionized distilled water was measured at 4° and 25°C for a period of 15 days.

2.3. In Vitro Release Study. The release characteristics of DsiRNA-CS NPs/complexes (CS concentration 0.3% w/v) were studied in PBS (pH 7.2). Samples (4 mL) were centrifuged at 35,000 rpm for 30 min at 25°C, and deionized water was replaced with buffer solution (3 mL). The mixture was placed on a magnetic stirrer with a stirring speed of 100 rpm at 37°C for 15 days. At different time intervals, samples were centrifuged at 35,000 rpm for 30 min at 25°C. Then, a whole volume of supernatant was removed for analysis and replaced with an equivalent volume of fresh buffer solution. The amount of released DsiRNA in the supernatant was analyzed by a UV-visible spectrophotometer (Shimadzu 1800) at a wavelength of 260 nm.

2.4. Cytotoxicity Study. The V79 and DLD-1 cells (ATCC, Manassas, USA) were cultured in DMEM and RPMI 1640 medium at cell density of 2 and 4×10^4 per well, respectively. Both cell lines were supplemented with 10% FBS 1% penstrep and maintained at 37°C in a humidified 5% CO_2 : 95% air atmosphere. At 24 and 48 h after incubation of DsiRNA-CS NPs or DsiRNA-CS complexes at 37°C, a final dilution of 1/10 per cell volume of alamarBlue reagent was added to the treated cells followed by a 4 h incubation prior to analysis. The absorbance of each sample at 570 nm (A570) was measured on a microplate reader (Varioskan Flash, Thermo Scientific, Waltham, MA, USA). Cell viability was determined by using the following equation:

$$\text{Cell viability (\%)} = \frac{A_{570} \text{ of treated cells}}{A_{570} \text{ of control cells}} \times 100. \quad (2)$$

2.5. Statistical Analysis. All the data were presented as mean ± standard deviation (SD). Data was analyzed with either the independent Student's t-test or analysis of variance (ANOVA), followed by post hoc Tukey's analysis) by using SPSS 19.0. For the independent t-test and ANOVA, differences between tested groups were considered significant when $P < 0.05$.

3. Results and Discussion

3.1. ATR-FTIR Spectroscopic Analysis. ATR-FTIR spectra of CS, TPP, naked DsiRNA, CS-TPP NPs, DsiRNA-CS NPs, and the DsiRNA-CS complexes are presented in Figure 2. The spectrum of CS (Figure 2(a)) shows characteristic peaks at 3430 cm^{-1} (–OH stretching), 2882 cm^{-1} (–CH stretching),

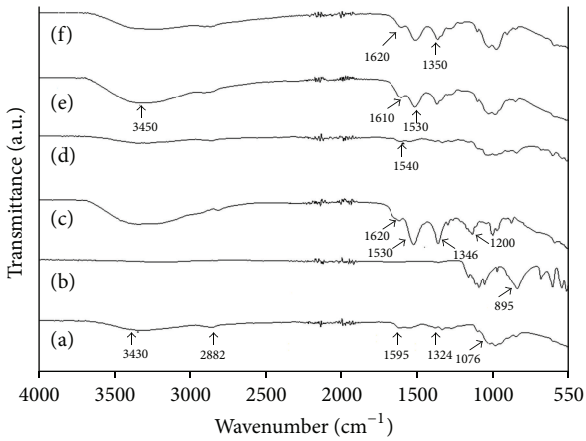

Figure 2: FTIR spectra containing 0.3% w/v CS. CS (a), TPP (b), DsiRNA (c), unloaded CS NPs (d), DsiRNA-CS NPs (e), and DsiRNA-CS complexes (f).

1595 cm^{-1} (–NH_2 stretching), 1324 cm^{-1} (C–N stretching), and 1076 cm^{-1} (C–O–C stretching). In the spectrum of TPP (Figure 2(b)), a characteristic peak is observed at 895 cm^{-1}. In the spectrum of DsiRNA (Figure 2(c)), characteristic P–CH_3 and P–CH_2 bending peaks are seen at 1346 cm^{-1} and 1530 cm^{-1}, respectively. Moreover, P=O stretching was observed in the region of 1200 cm^{-1}. Another peak for DsiRNA is seen at 1620 cm^{-1}. The spectrum of unloaded CS NPs showed characteristic peaks for CS and TPP, with slight shifting in the wavelengths and a decrease in intensity (Figure 2(d)). The peak for the N–H bending vibration at 1595 cm^{-1} shifted to 1540 cm^{-1} in the unloaded CS NPs after addition of TPP. In the spectrum for DsiRNA-CS NPs, characteristic peaks for CS, TPP, and DsiRNA were observed, which shows the presence of DsiRNA in CS NPs (Figure 2(e)). The –OH stretching was seen at 3450 cm^{-1}, which indicates CS. The peaks obtained at 1610 and 1530 cm^{-1} confirmed the presence, DsiRNA in the NPs. In the spectrum of the DsiRNA-CS complex, all characteristic peaks for CS and DsiRNA are seen (Figure 2(f)). Hence, FTIR spectra confirmed the successful preparation of the CS NPs, DsiRNA-CS NPs and DsiRNA-CS complexes.

3.2. Particle Size. The mean particle size of CS NPs loaded with DsiRNA prepared by either the simple complexation or adsorption method was significantly increased by increasing the concentration of CS from 0.1% to 0.4% w/v (ANOVA, Tukey's post-hoc analysis, $P < 0.05$). This was expected due to the decreased viscosity at the lower concentration of CS, which resulted in better solubility and properties consistent with the polyelectrolyte type of materials. This allowed for a more efficient interaction between negatively charged DsiRNA and the cationic CS; thus a smaller particle size was produced [18].

The CS-DsiRNA complexes had a larger particle size as compared to CS-DsiRNA NPs (independent Student's t-test, $P < 0.05$) as shown in Table 1. A larger particle size was expected due to the presence of intermolecular hydrogen bonding (due to –OH groups) and higher intermolecular electrostatic repulsion (due to –$NH3^+$ groups) that exists along the contour of CS [23]. The smaller size of CS NPs adsorbed with DsiRNA could be due to quick gelling of CS in contact with the polyanions (TPP) that relies on the formation of inter- and intramolecular cross-linkages mediated by the polyanions. NPs were formed immediately upon mixing the TPP and CS solutions, as molecular linkages were formed between the TPP phosphates and CS amino groups. This resulted in less electrostatic repulsion between the amino groups of CS due to TPP neutralization [24]. In addition, DsiRNA adsorption onto the surface of CS NPs was found to have no significant effect on the particle size of CS NPs.

3.3. Zeta Potential. The comparative positive surface charge (zeta potential) of the DsiRNA loaded CS NPs/complexes increased with increasing the concentration of CS at a constant DsiRNA concentration (ANOVA, Tukey's post-hoc analysis, $P < 0.05$) as shown in Table 1. This increase was due to the increase in the number of positive charges, which counteracts the negatively charged DsiRNA because the amount of DsiRNA was fixed. A net positive charge for the particles was desirable so as to prevent particle aggregation and promote electrostatic interaction with the overall negative charge of the cell membrane [25].

The surface charge of CS NPs (unloaded) ranged approximately from +40 to +60 mV (data not shown) by varying the CS concentration from 0.1% to 0.4% w/v. However, the addition of DsiRNA (15 μg/mL) to CS NPs showed a non-significant decrease in the zeta potential. This finding differed from that of the siRNA-CS NPs, which decreased in zeta potential after the adsorption process [18]. This was thought to be due to the larger size of the DsiRNA duplex (27 mer, MW 16,558 g/moL) as compared to the siRNA duplex (21 mer, MW 13,300 g/moL). In an equivalent volumetric solution of DsiRNA and siRNA, fewer units of DsiRNA than of siRNA would be present in solution because of the larger size of the DsiRNA (27 mer). As a result, a fewer number of negatively charged phosphate groups would be available in DsiRNA to compensate for the positive amine groups of the CS. In contrast, more, and smaller sized (21 mer), siRNA units (and therefore more phosphate groups) would be present in solution to compensate for the amine groups of CS. This observed behaviour was in accordance to the pDNA [26]. For this reason, CS NPs loaded with DsiRNA showed a more positive zeta potential than siRNA loaded CS NPs.

3.4. Morphology. The images of the CS NPs loaded with DsiRNA were obtained by TEM (Figure 3) and AFM (Figure 4). Figure 3(a) shows that unloaded CS NPs exhibited a spherical structure. The DsiRNA-CS NPs also had the spherical morphology as depicted in Figures 3(b), 3(d), 3(f), and 3(h). In contrast, DsiRNA-CS complexes exhibited irregular shapes (Figures 3(c), 3(e), 3(g), and 3(i)). AFM micrographs of 0.3% w/v CS also revealed a spherical morphology for DsiRNA-CS NPs (Figure 4(a)) and an irregular morphology for DsiRNA-CS complexes (Figure 4(b)). The heterogeneous

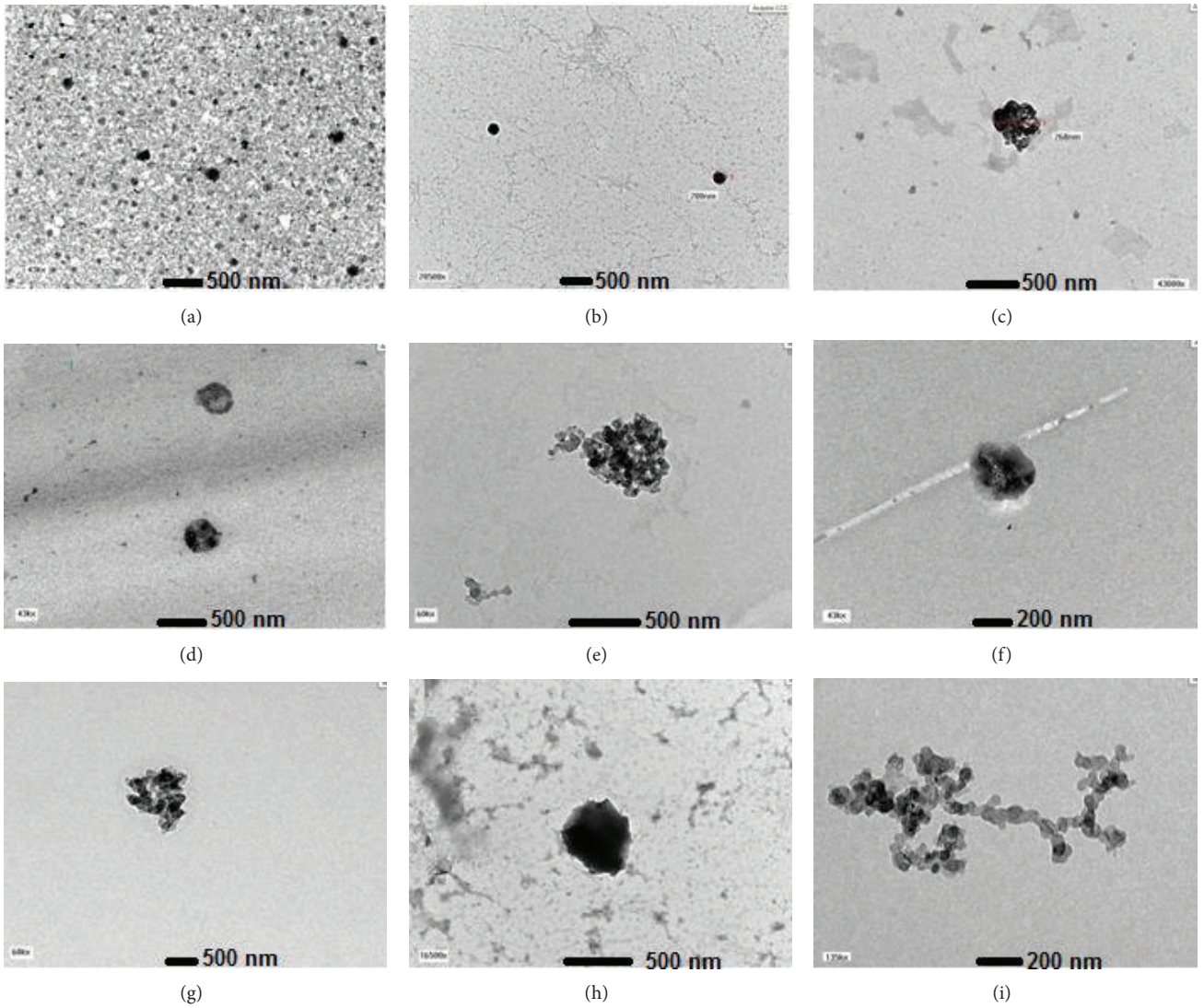

(a) (b) (c)

(d) (e) (f)

(g) (h) (i)

Figure 3: TEM images of NPs/complexes. Blank CS NPs (0.3% w/v CS) (a), DsiRNA-CS NPs ((b), (d), (f), and (h)), and DsiRNA-CS complexes ((c), (e), (g), and (i)) of 0.1%, 0.2%, 0.3%, and 0.4% w/v of CS, respectively. The magnification of the images were 43 kx ((a), (c), (d), and (f)), 60 kx ((e) and (g)), 20500x (b), 165 kx (h), and 135 kx (i).

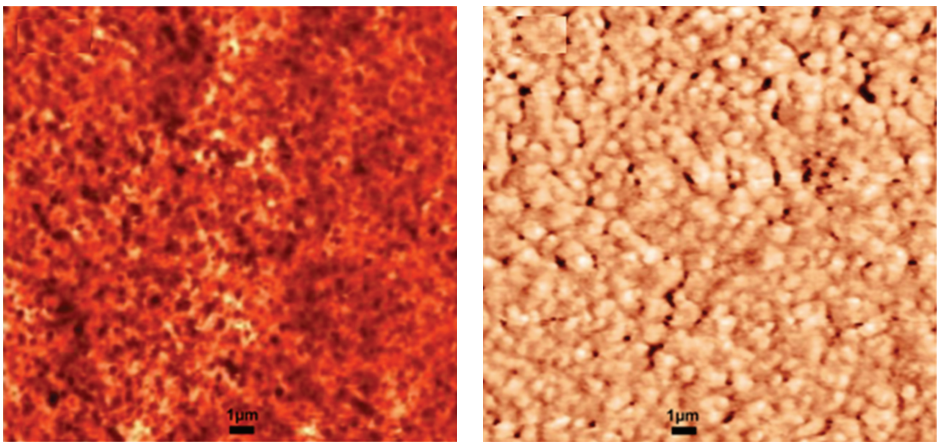

(a) (b)

Figure 4: AFM micrographs (containing 0.3% w/v CS). DsiRNA-CS NPs (a) and DsiRNA-CS complexes (b) at 1 μm scan size.

Table 1: Particle size, PDI, and zeta potential of DsiRNA-CS NPs/complexes, $n = 3$.

CS concentration (% w/v)	Simple complexation			Adsorption		
	Particle size (nm) ± SD	PDI ± SD	Zeta potential (mV) ± SD	Particle size (nm) ± SD	PDI ± SD	Zeta potential (mV) ± SD
0.1	270.33 ± 56.14	0.60 ± 0.06	+56.77 ± 7.64	216.37 ± 45.52	0.59 ± 0.06	+40.50 ± 2.95
0.2	404.13 ± 10.64	0.75 ± 0.17	+57.10 ± 6.22	231.00 ± 68.78	0.52 ± 0.18	+46.13 ± 4.21
0.3	624.67 ± 64.90	0.69 ± 0.08	+68.50 ± 1.87	251.23 ± 33.80	0.53 ± 0.10	+37.27 ± 6.07
0.4	734.40 ± 73.73	0.72 ± 0.19	+69.23 ± 5.05	336.50 ± 11.38	0.74 ± 0.12	+61.30 ± 4.91

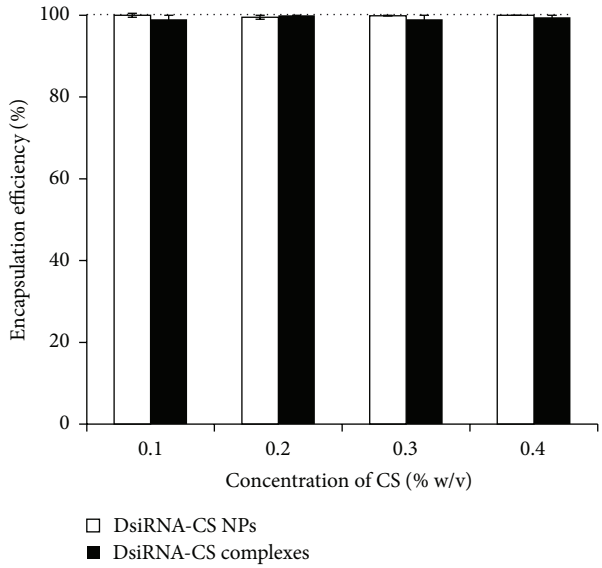

Figure 5: Encapsulation efficiency of DsiRNA-CS NPs/complexes containing different CS concentrations. 0.1% w/v CS (a), 0.2% w/v CS (b), 0.3% w/v CS (c), and 0.4% w/v CS (d).

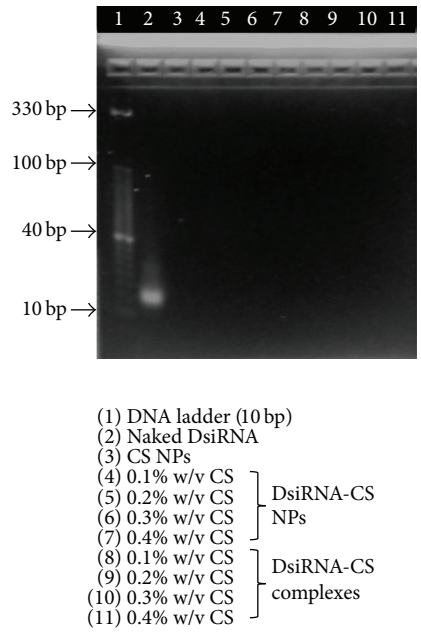

Figure 6: Binding efficiency of DsiRNA loaded CS NPs/complexes as determined by 4% w/v agarose gel electrophoresis.

morphology of DsiRNA-CS complexes obtained in this study was in agreement with previously reported studies on CS complexes [27, 28]. The particle morphology is an important factor for the colloidal and chemical stability. The results showed that DsiRNA-CS NPs remained more stable at different polymeric concentrations, resulting in spherical morphology, at different CS concentrations. On the other hand, DsiRNA-CS complexes showed less stability at different polymeric concentrations, resulting in aggregation and irregular morphology, at different CS concentrations. The difference in shape/stability between nanospheres and complexes may be best understood on the basis that the formation of CS NPs is governed not only by electrostatic interactions between the DsiRNA and CS but also by the interactions between TPP and CS. The latter interaction was responsible for the controlled gelation of CS in a nanoparticulate form. This controlled gelation and reticulation process could therefore explain why the resulting nanoparticles were more spherical, compact, and stable than the simple complexes [26].

3.5. DsiRNA Encapsulation and Binding Efficiency. A high DsiRNA encapsulation efficiency was obtained (100%) for DsiRNA loaded CS NPs/complexes as measured by spectrophotometry in Figure 5. For CS NPs/complexes loaded with DsiRNA, complete binding of DsiRNA to CS was observed (due to the absence of a trailing band), which demonstrates a strong interaction between CS and DsiRNA as shown in Figure 6. Overall, these results showed that DsiRNA was efficiently and tightly associated to the nanoparticles; however, it was not irreversibly bound since it could be released upon the degradation of the polymeric matrix [26, 29].

3.6. Storage Stability. The data corresponding to DsiRNA-CS NPs/complexes size progression over time is presented in Figure 7. The rationale for conducting this study in deionized water was in the interest of obtaining information about the NPs/complexes' stability in their suspending medium. This could help to avoid the need for extra procedures to stabilize the NPs/complexes, such as a lyophilization step. According to previous findings, cross-linking reactions have been described for improving the properties of the particulates [30]. The results of this study support the previous finding that DsiRNA-CS complexes without TPP tend to demonstrate some degree of size variation, although no statistical significance was seen at 4°C and 25°C, as shown in Figures 7(a) and 7(b), respectively. This was accompanied by an increase

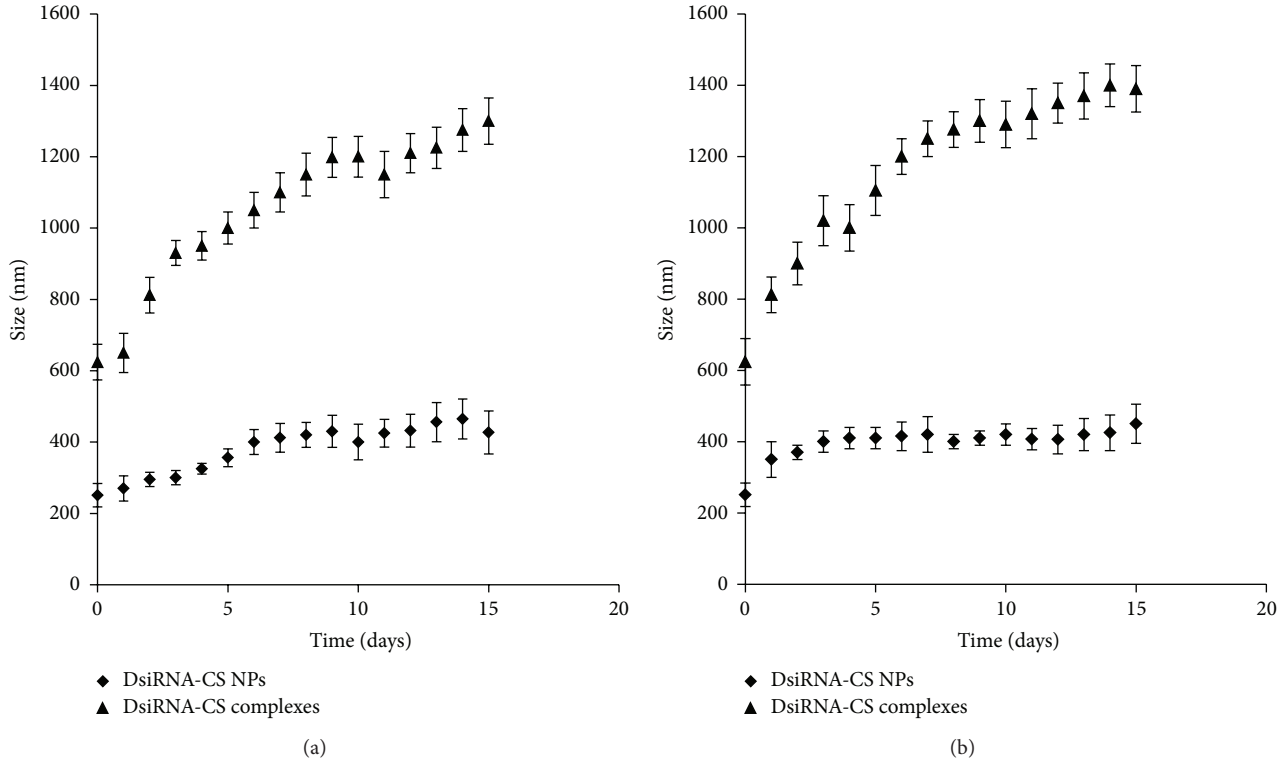

Figure 7: Stability study of DsiRNA-CS NPs/complexes at different temperature ranges. At 4°C (a) and 25°C (b), $n = 3$.

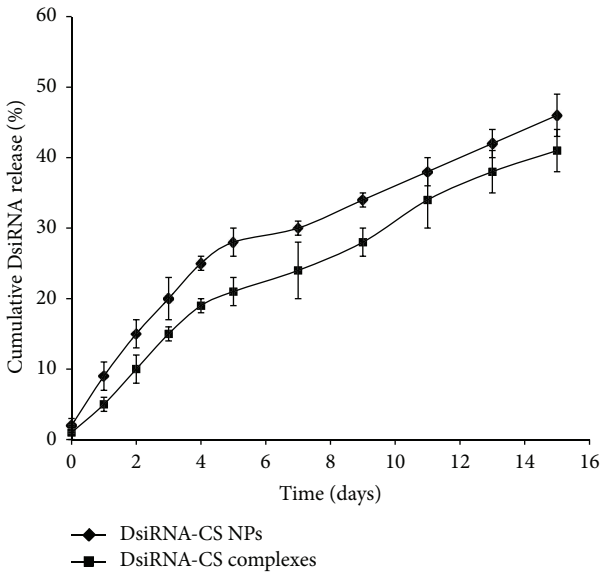

Figure 8: The release profile of DsiRNA loaded CS NPs/complexes at pH 7.2, $n = 3$.

in PDI after 15 days of storage. On the contrary, DsiRNA-CS NPs containing TPP had decent stability at both temperatures as shown in Figures 7(a) and 7(b), without a significant size variation during the experimental period of 15 days. The results for the DsiRNA-CS NPs indicate that TPP acts as a stabilizer, possibly because of its cross-linking effect, which causes polymeric molecules to establish stronger interactions with each other to form a more stable structure that is less prone to aggregation as reported elsewhere [31]. This suggests that DsiRNA-CS complexes behave as a metastable system, and thus they must be stored lyophilized, and fresh aqueous solutions should be prepared only when required. However, DsiRNA-CS NPs were stable at both temperatures, so they could be stored at 4° and 25°C without lyophilization.

3.7. In Vitro Release of DsiRNA. The *in vitro* release study of DsiRNA from CS NPs/complexes was carried out in PBS to confirm the success of DsiRNA loading and to understand the release mechanism and kinetics of DsiRNA from CS NPs/complexes. NPs/complexes prepared from a CS concentration of 0.3% w/v were selected as they had the desired characteristics (small nanosize, net positive charge, high entrapment, and binding efficiency). The *in vitro* release profiles of DsiRNA from the NPs/complexes were investigated for 15 days in PBS at pH of 7.2. Figure 8 illustrates that the release of DsiRNA could be divided into two stages based on the release rate (the slope of the release profile). In the first stage, the drug release pattern in DsiRNA-CS NPs/complexes showed a rapid release in the first 4 days resulting in a 25% and 19% cumulative release of DsiRNA in PBS (pH 7.2), respectively. The release of DsiRNA at this stage might involve the diffusion of DsiRNA bound at the particle surface. In the second stage, DsiRNA was released at a constant rate (sustained release) from CS NPs/complexes for up to 15 days. After 15 days, approximately 46% and 41% total recovered

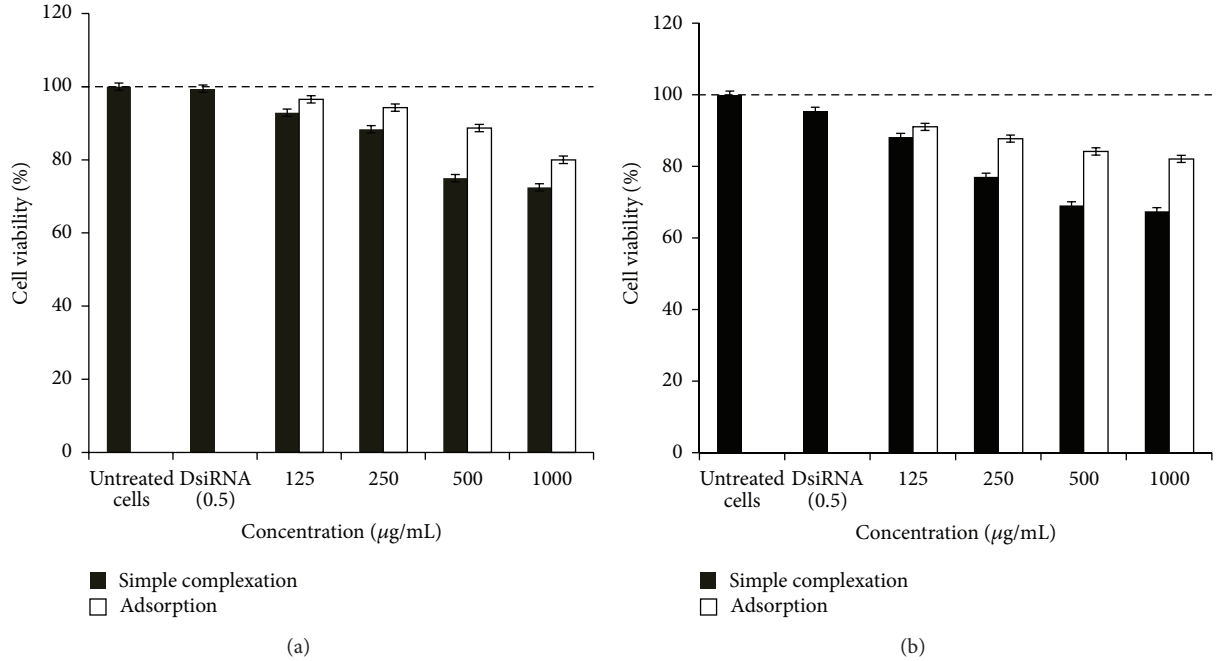

Figure 9: Cytotoxicity effect of DsiRNA loaded CS NPs/complexes on V79 cells. After 24 h (a) and 48 h (b), $n = 3$.

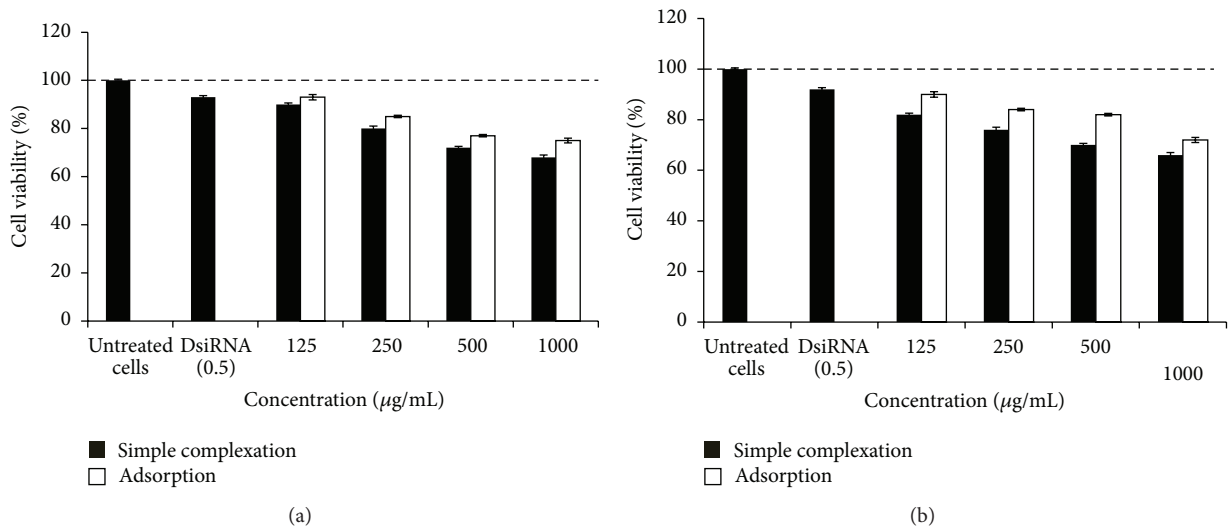

Figure 10: Cytotoxicity effect of DsiRNA loaded CS NPs/complexes on DLD-1 cells. After 24 h (a) and 48 h (b), $n = 3$.

amount of DsiRNA was released from CS NPs/complexes, respectively. However, no significant difference was observed in the DsiRNA cumulative amount released and in the release rate from CS NPs and the complexes. The nonsignificant difference in the cumulative amount released and in the release rate might be due to the fact that the dissolution rate of the polymer near the surface was high; therefore, the amount of drug release from the surface would also be high [32].

3.8. Cytotoxicity Study. To investigate the cytotoxic effect of DsiRNA-CS NPs/complexes on V79 and DLD-1 cells, an alamarBlue cell viability assay was performed. In V79 cells, over 85% cell viability was observed for DsiRNA-CS NPs in comparison to untreated cells (Figure 9). Naked DsiRNA did not show any loss of cell viability. However, 15–30% loss of cell viability was observed for CS-DsiRNA complexes. A significant difference was observed in the cytotoxicity of DsiRNA-CS NPs/complexes at 24 h and 48 h after incubation

(independent Student's t-test, $P < 0.05$). The DsiRNA-CS complexes exhibited more loss of cell viability than DsiRNA-CS NPs at 24 h after incubation (Figure 9(a)). The difference in the immediate cellular response between CS-DsiRNA NPs/complexes might be due to the greater positive zeta potential of the CS-DsiRNA complexes, which resulted in a stronger interaction between CS-DsiRNA complexes and a negatively charged cell membrane leading to more loss of cell viability. Similarly, DsiRNA-CS NPs/complexes showed a significant decrease in cell viability at 48 h after incubation as shown in Figure 9(b) (independent Student's t-test, $P < 0.05$). The cytotoxicity observed by both methods might be due to a high positive zeta potential in CS NPs/complexes that may interact with the negatively charged cell membrane. Moreover, DsiRNA-CS complexes showed greater loss of cell viability at 48 h after incubation than DsiRNA-CS NPs, which might be due to the greater positive zeta potential of the complexes that results in physiological stress to the cells.

On DLD-1 cells, DsiRNA-CS NPs/complexes exhibited cytotoxic activity at 24 h and 48 h after incubation (Figures 10(a) and 10(b)). Over a 15–35% and 10–28% loss in cell viability was observed for CS-DsiRNA/complexes, depending on the concentration used. An average of 7–8% loss in cell viability was observed for DsiRNA in comparison to untreated cells. No significant difference was observed in the cytotoxicity between DsiRNA CS NPs/complexes at 24 h and 48 h after incubation in DLD-1 cells as depicted in Figures 10(a) and 10(b), respectively. Both NPs and complexes loaded with DsiRNA showed a decrease in cell viability in DLD-1 and V79 cells, with DLD-1 cells having a slightly greater loss of cell viability. However, the difference in cell viability loss between DLD-1 and V79 cells by DsiRNA CS NPs/complexes was not significant. The reason behind this loss of cell viability in DLD-1 cells might be due to CS' ability to inhibit the growth of human cancer cells through an anti-angiogenic mechanism [33]. Further investigation in different cell lines is still ongoing to address this effect.

4. Conclusions

CS complexes and NPs loaded with DsiRNA were successfully synthesized by simple complexation and ionic gelation methods, respectively. FTIR analysis confirmed the successful encapsulation of DsiRNA onto/with CS NPs/complexes. CS NPs obtained from the ionic gelation method showed it to be a better method, as it produced smaller particles that are expected to be more suitable for the efficient delivery of DsiRNA to the target cells, improved storage stability at different temperatures, and lesser toxicity in normal cells. In contrast to that, DsiRNA-CS complexes exhibited larger particle size, were more prone to aggregation, and had higher toxicity for normal cells, which may be due to their higher positive zeta potential. Nonetheless, both methods exhibited sustained release of DsiRNA over a period of time and high binding and high encapsulation (100%) efficiencies. The results of the present study, therefore, suggest that CS NPs (ionic gelation) could be used as a biocompatible, nonviral gene delivery system. This study also presents a platform for further optimization studies of CS-based NPs, such as steric stabilization and targeting.

Conflict of Interests

The authors declare no conflict of interests with regard to the work.

Acknowledgments

The authors gratefully acknowledge the financial support of this research by Exploratory Research Grant Scheme (ERGS) with Grant no. ERGS/1/2011/SKK/UKM/02/11. The authors would like to thank all members of the Centre for Drug Delivery Research for their support.

References

[1] H. Katas, N. N. S. N. Dzulkefli, and S. Sahudin, "Synthesis of a new potential conjugated TAT-peptide-chitosan nanoparticles carrier via disulphide linkage," *Journal of Nanomaterials*, vol. 2012, Article ID 134607, 7 pages, 2012.

[2] K. Lundstrom, "Latest development in viral vectors for gene therapy," *Trends in Biotechnology*, vol. 21, no. 3, pp. 117–122, 2003.

[3] S.-D. Li and L. Huang, "Non-viral is superior to viral gene delivery," *Journal of Controlled Release*, vol. 123, no. 3, pp. 181–183, 2007.

[4] S. H. Kim, H. Mok, J. H. Jeong, S. W. Kim, and T. G. Park, "Comparative evaluation of target-specific GFP gene silencing efficiencies for antisense ODN, synthetic siRNA, and siRNA plasmid complexed with PEI-PEG-FOL conjugate," *Bioconjugate Chemistry*, vol. 17, no. 1, pp. 241–244, 2006.

[5] M. Hashida, S. Takemura, M. Nishikawa, and Y. Takakura, "Targeted delivery of plasmid DNA complexed with galactosylated poly (L-lysine)," *Journal of Controlled Release*, vol. 53, no. 1–3, pp. 301–310, 1998.

[6] E. Kleemann, M. Neu, N. Jekel et al., "Nano-carriers for DNA delivery to the lung based upon a TAT-derived peptide covalently coupled to PEG-PEI," *Journal of Controlled Release*, vol. 109, no. 1–3, pp. 299–316, 2005.

[7] J. H. Felgner, R. Kumar, C. N. Sridhar et al., "Enhanced gene delivery and mechanism studies with a novel series of cationic lipid formulations," *Journal of Biological Chemistry*, vol. 269, no. 4, pp. 2550–2561, 1994.

[8] F. Liu and L. Huang, "Development of non-viral vectors for systemic gene delivery," *Journal of Controlled Release*, vol. 78, no. 1–3, pp. 259–266, 2002.

[9] H. Katas, Z. Hussain, and T. C. Ling, "Chitosan nanoparticles as a percutaneous drug delivery system for hydrocortisone," *Journal of Nanomaterials*, vol. 2012, Article ID 372725, 11 pages, 2012.

[10] A. G. Luque-Alcaraz, J. Lizardi, F. M. Goycoolea et al., "Characterization and antiproliferative activity of nobiletin-loaded chitosan nanoparticles," *Journal of Nanomaterials*, vol. 2012, Article ID 265161, 7 pages, 2012.

[11] M. N. Kumar, R. A. Muzzarelli, C. Muzzarelli, H. Sashiwa, and A. J. Domb, "Chitosan chemistry and pharmaceutical perspectives," *Chemical Reviews*, vol. 104, no. 12, pp. 6017–6084, 2004.

[12] K. M. Vårum, M. M. Myhr, R. J. N. Hjerde, and O. Smidsrød, "In vitro degradation rates of partially N-acetylated chitosans in human serum," *Carbohydrate Research*, vol. 299, no. 1-2, pp. 99–101, 1997.

[13] S. B. Rao and C. P. Sharma, "Use of chitosan as a biomaterial: studies on its safety and hemostatic potential," *Journal of Biomedical Materials Research*, vol. 34, pp. 21–28, 1997.

[14] M. J. Alonso and A. Sánchez, "The potential of chitosam in ocular drug delivery," *Journal of Pharmacy and Pharmacology*, vol. 55, no. 11, pp. 1451–1463, 2003.

[15] K. Y. Lee, "Chitosan and its derivatives for gene delivery," *Macromolecular Research*, vol. 15, no. 3, pp. 195–201, 2007.

[16] S. Gao, J. Chen, L. Dong, Z. Ding, Y.-H. Yang, and J. Zhang, "Targeting delivery of oligonucleotide and plasmid DNA to hepatocyte via galactosylated chitosan vector," *European Journal of Pharmaceutics and Biopharmaceutics*, vol. 60, no. 3, pp. 327–334, 2005.

[17] H. Katas and H. O. Alpar, "Development and characterisation of chitosan nanoparticles for siRNA delivery," *Journal of Controlled Release*, vol. 115, no. 2, pp. 216–225, 2006.

[18] W. Fan, W. Yan, Z. Xu, and H. Ni, "Formation mechanism of monodisperse, low molecular weight chitosan nanoparticles by ionic gelation technique," *Colloids and Surfaces B*, vol. 90, no. 1, pp. 21–27, 2012.

[19] D. Siolas, C. Lerner, J. Burchard et al., "Synthetic shRNAs as potent RNAi triggers," *Nature Biotechnology*, vol. 23, no. 2, pp. 227–231, 2005.

[20] D.-H. Kim, M. A. Behlke, S. D. Rose, M.-S. Chang, S. Choi, and J. J. Rossi, "Synthetic dsRNA Dicer substrates enhance RNAi potency and efficacy," *Nature Biotechnology*, vol. 23, no. 2, pp. 222–226, 2005.

[21] S. D. Rose, D.-H. Kim, M. Amarzguioui et al., "Functional polarity is introduced by Dicer processing of short substrate RNAs," *Nucleic Acids Research*, vol. 33, no. 13, pp. 4140–4156, 2005.

[22] P. Calvo, C. R. López, J. L. Vila-Jato, and M. J. Alonso, "Novel hydrophilic chitosan-polyethylene oxide nanoparticles as protein carriers," *Journal of Applied Polymer Science*, vol. 63, no. 1, pp. 125–132, 1997.

[23] G. Qun and W. Ajun, "Effects of molecular weight, degree of acetylation and ionic strength on surface tension of chitosan in dilute solution," *Carbohydrate Polymers*, vol. 64, no. 1, pp. 29–36, 2006.

[24] Q. Gan, T. Wang, C. Cochrane, and P. McCarron, "Modulation of surface charge, particle size and morphological properties of chitosan-TPP nanoparticles intended for gene delivery," *Colloids and Surfaces B*, vol. 44, no. 2-3, pp. 65–73, 2005.

[25] R. M. Schiffelers, M. C. Woodle, and P. Scaria, "Pharmaceutical Prospects for RNA Interference," *Pharmaceutical Research*, vol. 21, no. 1, pp. 1–7, 2004.

[26] N. Csaba, M. Köping-Höggård, and M. J. Alonso, "Ionically crosslinked chitosan/tripolyphosphate nanoparticles for oligonucleotide and plasmid DNA delivery," *International Journal of Pharmaceutics*, vol. 382, no. 1-2, pp. 205–214, 2009.

[27] M. Köping-Höggård, Y. S. Mel'nikova, K. M. Vårum, B. Lindman, and P. Artursson, "Relationship between the physical shape and the efficiency of oligomeric chitosan as a gene delivery system in vitro and in vivo," *Journal of Gene Medicine*, vol. 5, no. 2, pp. 130–141, 2003.

[28] P. Erbacher, S. Zou, T. Bettinger, A.-M. Steffan, and J.-S. Remy, "Chitosan-based vector/DNA complexes for gene delivery: biophysical characteristics and transfection ability," *Pharmaceutical Research*, vol. 15, no. 9, pp. 1332–1339, 1998.

[29] M. E. Martin and K. G. Rice, "Peptide-guided gene delivery," *AAPS Journal*, vol. 9, no. 1, article 3, pp. E18–E29, 2007.

[30] F.-L. Mi, H.-W. Sung, S.-S. Shyu, C.-C. Su, and C.-K. Peng, "Synthesis and characterization of biodegradable TPP/genipin co-crosslinked chitosan gel beads," *Polymer*, vol. 44, no. 21, pp. 6521–6530, 2003.

[31] S. Rodrigues, A. M. R. Costa, and A. Grenha, "Chitosan/carrageenan nanoparticles: effect of cross-linking with tripolyphosphate and charge ratios," *Carbohydrate Polymers*, vol. 89, no. 1, pp. 282–289, 2012.

[32] L. Keawchaoon and R. Yoksan, "Preparation, characterization and in vitro release study of carvacrol-loaded chitosan nanoparticles," *Colloids and Surfaces B*, vol. 84, no. 1, pp. 163–171, 2011.

[33] Y. Xu, Z. Wen, and Z. Xu, "Chitosan nanoparticles inhibit the growth of human hepatocellular carcinoma xenografts through an antiangiogenic mechanism," *Anticancer Research*, vol. 30, no. 12, pp. 5103–5109, 2009.